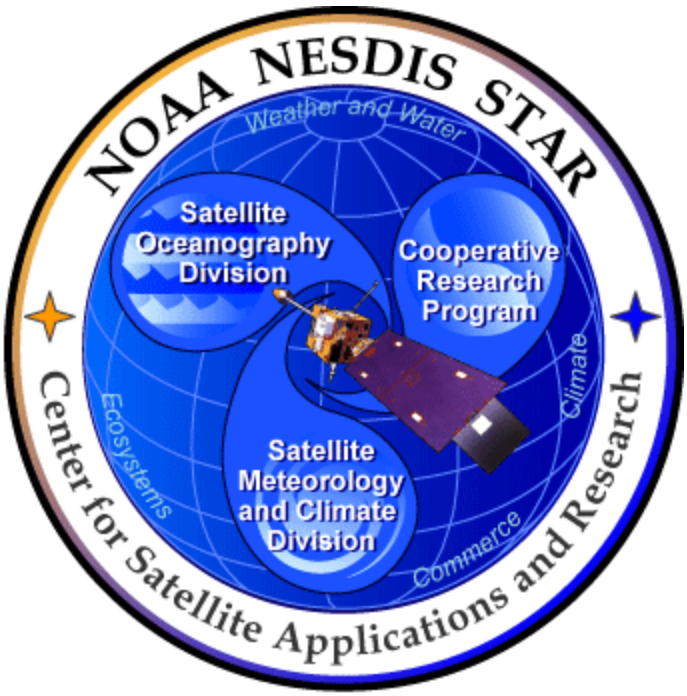

NOAA NESDIS
CENTER for SATELLITE APPLICATIONS and RESEARCH

NUCAPS Outgoing Longwave Radiation Algorithm Theoretical Basis Document

Prepared by
Kexin Zhang (IMSG), Quanhua Liu (STAR)

Kexin.zhang@noaa.gov

Version 1.0

October 6, 2016

DOCUMENT HISTORY
DOCUMENT REVISION LOG

The Document Revision Log identifies the series of revisions to this document since the baseline release. Please refer to the above page for version number information.

DOCUMENT TITLE: Algorithm Theoretical Basis Document			
DOCUMENT CHANGE HISTORY			
Revision No.	**Date**	**Revision Originator Project Group**	**CCR Approval # and Date**
1.0	N/A	No version 1	N/A

LIST OF CHANGES

Significant alterations made to this document are annotated in the List of Changes table.

DOCUMENT TITLE: Algorithm Theoretical Basis Document					
LIST OF CHANGE-AFFECTED PAGES/SECTIONS/APPENDICES					
Version Number	**Date**	**Changed By**	**Page**	**Section**	**Description of Change(s)**

TABLE OF CONTENTS

LIST OF TABLES

LIST OF FIGURES

LIST OF ACRONYMS

ADM	Angular Directional Model
ADL	Algorithm Development Library
AIRS	Atmospheric Infrared Sounder
AIT	Algorithm Integration Team
ASDC	Atmospheric Science Data Center
ATBD	Algorithm Theoretical Basis Document
AVHRR	Advanced Very High Resolution Radiometer
CERES	The Cloud and the Earth's Radiant Energy System
CLASS	Comprehensive Large Array-data Stewardship System
CrIS	Cross-track Infrared Sounder
CV	Coefficient of Variation
EBMs	Energy Balance Models
ERBE	Earth Radiation Budget Experiment
FOV	Field of View
GCMs	General Circulation Models
GES DISC	NASA Goddard Earth Sciences Data and Information Service Center
HIRS	High-resolution Infrared Sounder
JPSS	Joint Polar Satellite System
IASI	Infrared Atmospheric Sounding Interferometer
ITCZ	Intertropical Convergence Zone
OLR	Outgoing Longwave Radiation
NUCAPS	NOAA Unique CrIS/ATMS Product Processing System
RTA	Radiative Transfer Algorithms
SDR	Sensor Data Record
SSF	CERES single scanner footprint
TOA	Top of Atmosphere
TRMM	Tropical Rainfall Measurement Mission

1. INTRODUCTION

Long-term measurements of outgoing longwave radiation (OLR) are essential for quantitatively understanding climate in terms of the earth's radiative energy budget within energy balance models (EBMs) and higher order general circulation models.
OLR has been widely used as a proxy for tropical convection and precipitation, particularly in diagnosing and understanding tropical intraseasonal to interannual variability and monsoons. The trends of OLR have been used to study the climate feedbacks and processes. Clouds and the Earth's Radiant Energy System (CERES) was designed to extend the Earth Radiation Budget Experiment (ERBE) data record of TOA longwave (LW) and shortwave (SW) fluxes. Since the infrared (IR) radiance measured in space by radiometers and spectrometers is part of the outgoing LW flux, there have been methods to estimate the OLR by combining radiance observations in several spectral regions. For example, a single IR window channel radiance (10 -- 12 μm) from the Advanced Very High Resolution (AVHRR) was used to estimate the OLR. By adding water vapor variance, the two-channel technique was applied to calculate the OLR from the geostationary satellite Meteosat 2. A multi-spectral OLR estimation method was using narrowband radiance observations from the High-resolution Infrared Sounder (HIRS) to estimate TOA total longwave flux. Vigorous validation efforts were performed for the HIRS multi-spectral OLR estimation technique against broadband observations derived from the ERBE and the CERES. These studies have showed that this OLR estimation algorithm can reliably achieve with an accuracy of about 4 to 8 Wm^{-2}, with biases that are within the respective radiometric accuracy of the reference instruments.

Beginning in 2002, the Atmospheric Infrared Sounder (AIRS) onboard Aqua in PM orbit has obtained high resolution IR spectra, followed by the Infrared Atmospheric Sounding Interferometer (IASI) onboard Metop-A/B in AM orbit since 2006/2012 and the Cross-track Infrared Sounder (CrIS) onboard Suomi-NPP in PM orbit since 2011. These combined satellite sounding systems are expected to provide a long-term record of high resolution radiance spectra. A method for estimating top-of-atmosphere (TOA) OLR from AIRS radiance measurements was thus subsequently developed by Sun et.al. It should be noted that the method is different from the AIRS Science Team Version-5 OLR products, which is computed as a function of the AIRS retrieved geophysical parameters. In this work we use CERES Aqua as an absolute reference for all of our
hyperspectral IR OLR products, regardless if they are from AIRS, IASI or CrIS, enabling the creation of consistent and stable OLR records from hyperspectral IR sounders. We therefore use AIRS as a transfer instrument with CERES Aqua OLR to estimate OLR from IASI and CrIS on a near real-time basis, this paper will focus on the algorithm for operational CrIS OLR estimation.

1.1. Product Overview

1.1.1. Product Description

This study describes the algorithm for deriving near real-time Outgoing Longwave Radiation (OLR) from Cross-track Infrared Sounder (CrIS) hyperspectral infrared sounder radiance measurements. The estimation of OLR on a near real-time basis provides a unique perspective for studying the variability of the Earth's current atmospheric radiation budget. CrIS derived OLR values are estimated as a weighted linear combination of CrIS adjusted “pseudo-channel" radiances. The algorithm uses Atmospheric Infrared Sounder (AIRS) as the transfer instrument, and a least-squares regression algorithm is applied to generate two sets of regression coefficients. The first set of regression coefficients is derived from collocated Clouds and the Earth's Radiant Energy System (CERES) OLR on Aqua and pseudo-channel radiances calculated from AIRS radiances. The second set of coefficients is derived to adjust the CrIS pseudo-channel radiance to account for the differences in pseudo-channel radiances between AIRS and CrIS. The CrIS-derived OLR is then validated by using a limited set of available CERES S-NPP OLR observations over 1deg lat/lon global grids, as well as monthly OLR mean and interannual differences against CERES OLR data sets from S-NPP and Aqua. The results show that the bias of global CrIS OLR estimation is within 2 Wm^{-2}, and the standard deviation is within 5 Wm^{-2} for all conditions, and 1 Wm^{-2} and 3 Wm^{-2} for homogeneous scenes. The interannual CrIS derived OLR differences agree well with Aqua CERES interannual OLR differences on a 1Deg lat/lon spatial scale, with only a small drift of the global mean of these two data sets of around 0.004 Wm^{-2}.

1.1.2. Product Requirements

Name	**Outgoing Longwave Radiation at TOA**
User	**NOAA CPC**
Geographic Coverage	**Nearly global**
Vertical Resolution	**N/A**
Horizontal Resolution	**25 km at nadir**
Product Refresh Rate/Coverage Time	**3 minutes**
Measurement Range	**0–500 Wm^{-2}**

Measurement Accuracy	**5 Wm^{-2}**
Measurement Precision	**12 Wm^{-2}**

Table 1-1 CrIS OLR requirement

1.2. Satellite Instrument Description

NUCAPS is a product system operated within the NDE DHS by OSPO. NUCAPS uses data from the Cross-track Infrared Sounder (CrIS) and the Advanced Technology Microwave Sounder (ATMS) instruments on the NPOESS Preparatory Project (NPP) platform. NPP launched on October 28, 2011. It is in a sun synchronous circular orbit with a 10:30am descending-node orbit at an altitude of 824 km.

CrIS is a Michelson Interferometer with 1305 channels measuring in the Infrared (IR) portion of the spectrum. It has the following spectral characteristics:

Spectral bands:
LWIR Band 650-1095 cm^{-1}
MWIR Band 1210-1750 cm^{-1}
SWIR Band 2155-2550 cm^{-1}

Spectral Resolution:
LWIR Band <0.625cm^{-1}
MWIR Band <1.25cm^{-1}
SWIR Band <2.50cm^{-1}

The CrIS instrument starts a new Earth scan every 8 seconds. Each scans contains 30 Fields of Regard (FOR) viewed on the Earth's surface with a scan width of ±50˚. Each FOR contains a simultaneously measured 3X3 set of Fields of View (FOVs). The CrIS FOVs are circular and have a diameter of 14 km at nadir.

2. ALGORITHM DESCRIPTION

2.1. Processing Outline

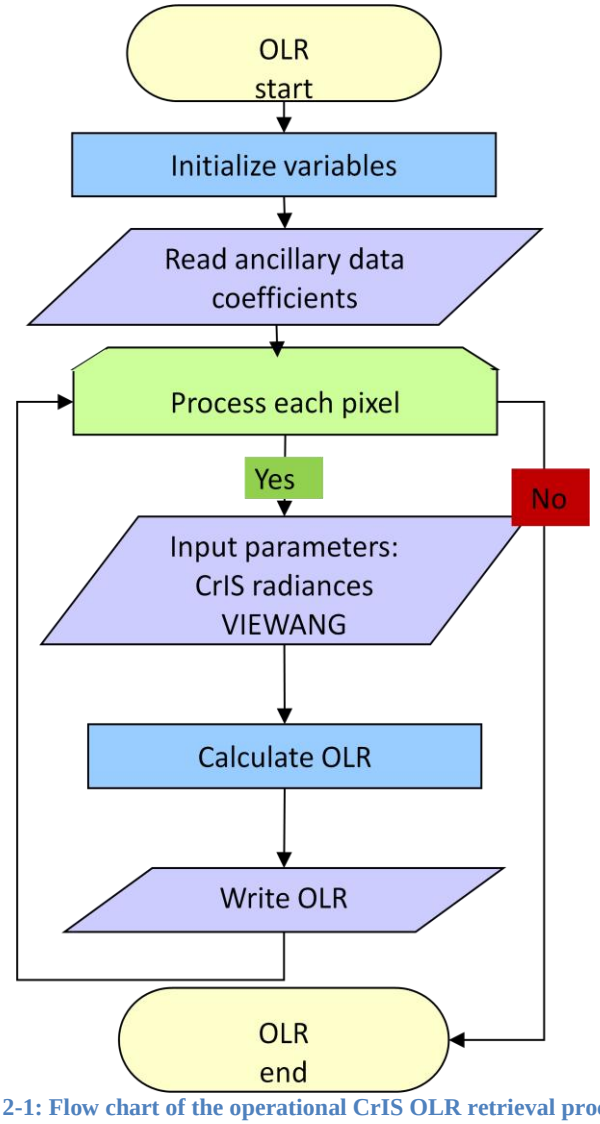

Figure 2-1: Flow chart of the operational CrIS OLR retrieval procedure.

2.2. Algorithm Input

For each pixel, the sensor inputs are apodized CrIS radiance with unit **(mWm^{-2} $(cm^{-1}$ $sr)^{-1}$),** view angles in degree and sensor quality flags. The static ancillary data have been saved in the operational NOAA Unique CrIS/ATMS Product Processing System (NUCAPS) preprocessor. These non-CrIS static data include parameters of 17 pseudo channels, OLR regression coefficients, radiance correction coefficients.

Table 2-1 OLR products inputs

Name	Type	Description	Dimension
Parameters of Pseudo Channel	**input**	**Start, end and center wavenumber**	**Floating number Array (17, 3)**
		List of IASI/CrIS channels	**integer number (17, nch)**
		Weights	**Floating number (17, nch)**
OLR Regression Coefficient	**input**	**CrIS OLR regression coefficients**	**Floating number array(18,8)**
Radiance correction coefficient	**input**	**CrIS to AIRS pseudo channel radiance correction regression coefficients**	**Floating number array(18, nch)**

2.3. Theoretical Description

The longwave radiation spectrum is the result of the combination of surface thermal emission and atmospheric absorption and thermal emission. Radiances across the spectrum are spectrally correlated; therefore, the variance of the spectrum can, to certain degree, be estimated with radiances sampled at several key frequencies. This forms the basis for narrow to broadband conversion. To avoid AIRS spectral gaps and “bad" channels, which may have NEDT > 2K at the reference temperature of 250 K, we reduced AIRS and CrIS radiance spectra into a small set of “pseudo-channels". A pseudo-channel is an ideal band-pass filter whose spectral response function equals to one in the spectral range of the pseudo-channel but zero elsewhere. We use 1567 (out of 2378) AIRS channels and 1004 (out of 1305) CrIS channels for the pseudo-channels. For each pseudo-channel *i*, the spectrally convolved radiance R given by

$$R(i,\theta) = \frac{1}{\nu_{2i} - \nu_{1i}} \int_{\nu_{1i}}^{\nu_{2i}} r(\nu,\theta) d\nu$$

where *i* is the index of the pseudo-channel, θ is view angle, ν_{1i} and ν_{2i} are the spectral band pass limits of the pseudo-channel *i*, $r(\nu,\theta)$ is the radiance at quasi-monochromatic wavenumber ν and θ. It is a simple trapezoidal numerical integral of AIRS and CrIS radiance. Figure 1 shows the spectral range of 17 pseudo channels within CrIS and AIRS radiance spectra. The center wavenumber (cm^{-1}) and width (cm^{-1}) of the pseudo channels are listed in table 2-3.

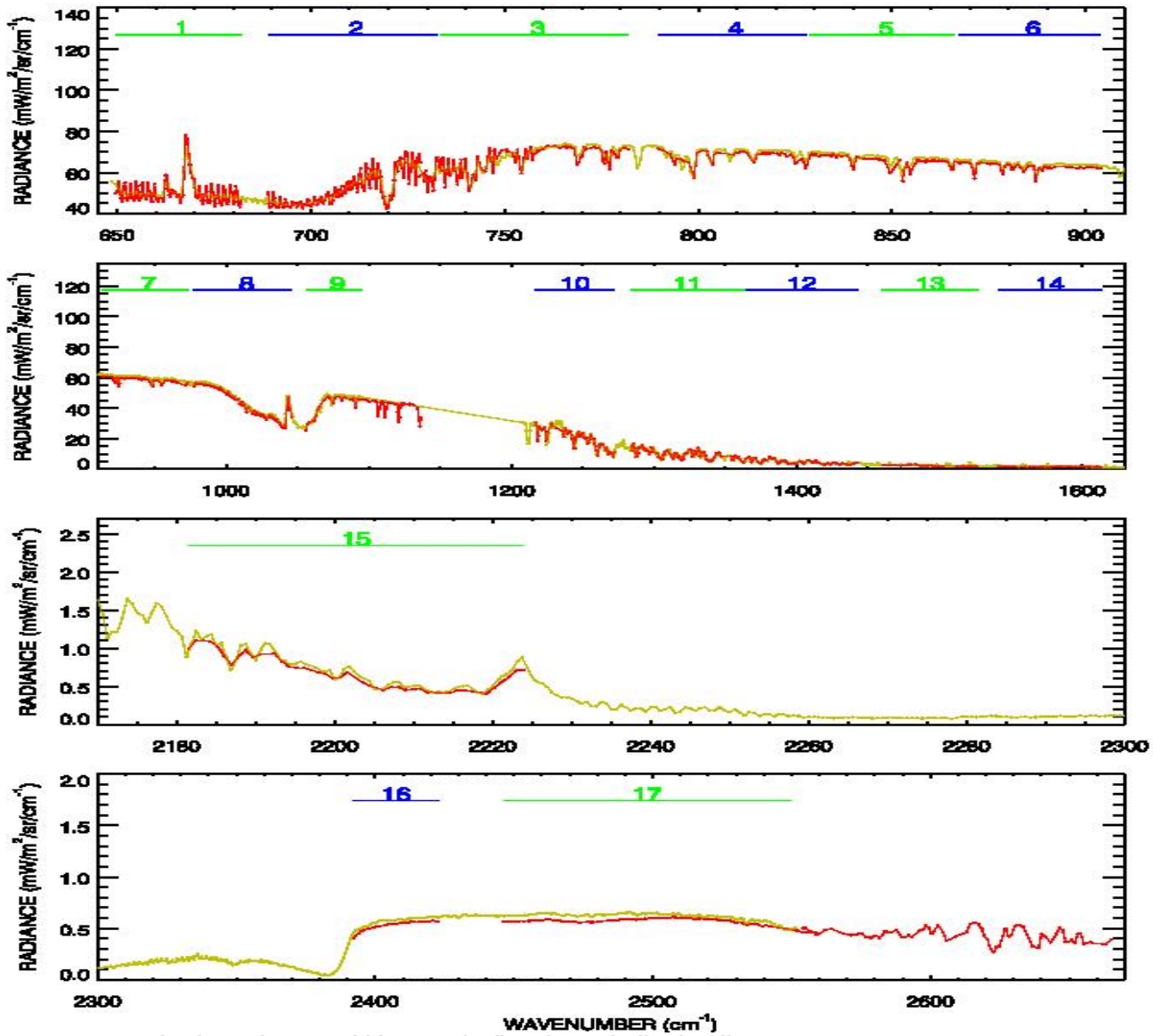

Figure 2-2 Pseudo channel range within AIRS (red) and CrIS (yellow) radiance spectra.

Pseudo-channel	Center wavenumber (cm^{-1})	Width (cm^{-1})	No. of CrIS channels	No. of AIRS channels
1	665.81	32.37	52	124
2	710.79	43.68	70	151
3	757.71	48.35	78	88
4	808.68	38.68	61	52
5	847.70	37.57	60	67
6	885.45	36.66	59	64
7	943.04	60.06	96	77
8	1011.43	69.53	111	107
9	1075.52	38.89	62	45
10	1244.78	55.61	45	80
11	1323.68	78.67	63	119
12	1403.84	78.47	63	121
13	1493.64	66.74	53	83
14	1577.48	72.77	59	77
15	2202.71	42.44	17	42
16	2407.46	30.78	13	29
17	2497.91	103.42	41	94

Table 2-2 Selection of AIRS and CrIS channels in 17 pseudo-channels.

The spectrally convolved radiances calculated in this manner are different between AIRS and CrIS. Reasons for this include the spectral resolution, instrument line shape and instrument radiometric noise used in the forward model. In real observations, different spatial sampling rates, sizes and shapes of footprints, and observing time differences might also be the reason to cause the discrepancies. Therefore, for each pseudo-channel, the radiance difference ΔR between AIRS and CrIS pseudo-channel radiances is adjusted by

$$\Delta R(i) = a_0 + \sum_{k=1}^{K} a_k \cdot r_{CrIS}(\nu_k)$$

The regression coefficients ak are trained by comparing AIRS and CrIS simulated radiances using the AIRS and CrIS fast forward radiative transfer algorithms (RTA) given “noaa89" sounding collections (7622 sounding profiles representing all sky conditions). The cloud height and fraction come from Pathfinder ATOVS (HIRS + MSU) retrievals that were co-located in time and space. Clouds are assumed as blackbody except for cirrus, which have a spectral-dependent non-unity emissivity. The view angle dependence of radiance is simulated at 90 view angles, from -49.43o to 49.43o. After deriving the adjustment coefficients in this manner, is applied to the CrIS measured radiances in each pseudo-channel to generate adjusted pseudo-channel radiances. The CrIS OLR is then derived as a linear combination of these adjusted pseudo-channel radiances. In the operational NOAA Unique CrIS/ATMS Product Processing System (NUCAPS) preprocessor, the adjustment coefficients and pseudo-channel parameters (which include start, end and center wavenumber and list of CrIS channels and weights) are saved as static ancillary data.
Since the AIRS and CERES instruments are on board EOS Aqua, and CrIS and CERES are on Suomi-NPP, the collocation of AIRS and CERES measurements only needs to be implemented in the spatial domain without considering the observation time difference. Sun et al. introduced the methodology of the collocation in a “big box", which includes 6 × 5 array of AIRS FOVs. Averaging CERES OLR and AIRS radiances in the “big box" will minimize the effect of the differences in the view and scanning properties of the two instruments. The coefficient of variation (CV) of CERES OLR in the big box is defined as the ratio of standard deviation divided by the mean. Any box with CV ≤ 5 is considered as a uniform scene, and is included in the training data sets. The training data sets are selected from one full day each month in

2006 for both AIRS level 1b and CERES FM3 Edition3A SSF data sets. The least squares regression algorithm relates the collocated CERES longwave fluxes to AIRS spectrally convolved radiances. The regression coefficients are trained in eight zenith view angle ranges to account for view angle dependence of AIRS and CrIS radiances. Applying those regression coefficients into adjusted CrIS spectrally convolved radiances, we get the estimated CrIS OLR in each FOV.

$$\hat{F}_{CrIS} = b_0(j) + \sum_{i=1}^{n} b(i,j) \cdot [R(i,\theta_j) + \Delta R(i)]$$

here n=17 and j represents one of the eight CrIS viewing angle bins. The 17 pseudo channels are built with the intention to use all of the available information content of both AIRS and CrIS radiance observations. This methodology then allows the estimation of CrIS OLR in each FOV directly from CrIS radiance observations in a simple, robust and fast way.

2.4. Algorithm Output

NUCAPS generate OLR in netCDF format for each granule, which includes the following variables for each FOV. NUCAPS shall generate 0.5X2.0 degree daily global grids of the outgoing longwave radiation product (NUCAPS OLR). There shall be separate files for ascending and descending data.

Table 2-3 OLR products outputs

Name	Type	Description	Dimension
Lat	**output**	**Latitudes of each FOV**	**Floating number array(4,30,9)**
Lon	**output**	**Longitudes of each FOV**	**Floating number array(4,30,9)**

Time	**output**	**UTC time as milliseconds from 1/1/1970**	**Double number array(4,30,9)**
SATZEN	**output**	**Satellite zenith angle for each FOV**	**Floating number array(4,30,9)**
SATHEIGHT	**output**	**Satellite height for each FOV**	**Floating number array(4,30,9)**
VIEWANG	**output**	**CrIS view angles for each FOV**	**Floating number array(4,30,9)**
FLUX	**output**	**Estimated CrIS OLR at TOA**	**Floating number array(4,30,9)**
QA	**output**	**CrIS OLR quality flag**	**Floating number array(4,30,9)**
AD_FLAG	**output**	**CrIS OLR acceding/descending indicator**	**Floating number array(4,30,9)**

2.5. Performance Estimates

2.5.1. Test Data Description

CERES SSF archived data products

- Single Scanner Footprint TOA/Surface Fluxes and Clouds (SSF) product files each contain one hour of instantaneous CERES data obtained from the Atmospheric Science Data Center (ASDC) at NASA Langley Research Center. https://eosweb.larc.nasa.gov/HORDERBIN/HTML_Start.cgi

- CERES Aqua FM3 Edition3A SSF products
- CERES SNPP FM5 Edition1A SSF products
- Merge the 24 hour boxes into 2 bins for ascending and descending orbits, respectively.
- Averaged CERES OLR at 1deg lat/lon grids.

CrIS SDR data

- Hamming apodization performed by NUCAPS preprocessor.
- Applied CrIS OLR algorithm to calculate CrIS OLR for each FOV.
- Merged CrIS OLR into 2 bins per day, one for all of the ascending orbits and the other for all of the descending orbits.
- Averaged CrIS OLR at 1deg lat/lon grids.

2.5.2. Sensor Effects

Quality control flags will be checked and inherited from the sensor input data for handling these exceptions

- Bad sensor input data (depending on what input QC available)
- Missing sensor input data
- Algorithm can't be run if any of the needed channel data are bad or missing

2.5.3. Retrieval Errors

To validate the accuracy and precision of CrIS derived CERES-like OLR (hereinafter referred to as CrIS OLR), we use available CERES outgoing longwave radiation fluxes from Suomi-NPP (hereinafter referred to as S-NPP CERES OLR) and from Aqua (hereinafter referred to as Aqua CERES OLR) platforms.
The daily OLR data can identify the variations in tropical clouds and rainfall that drive global weather patterns. Simultaneous CERES broadband measurements for S-NPP are the best candidate to validate the CrIS OLR algorithm.

Due to the difference of the spectral range and spatial resolution of these two instruments, we average CERES and CrIS OLR on a 1o×1o latitude-longitude grid. The daily global grid OLR bias is near 1 Wm^{-2} and the standard deviation is near 5 Wm^{-2}. We calculated monthly means for April 2013 and April 2014 respectively, for S-NPP CERES, Aqua CERES and CrIS derived OLR. The statistical results are shown in Table 2-4.

Table 2-4 Statistical results for monthly and interannual OLR comparison.

Monthly mean	**(CrIS – CERES Aqua) OLR (W/m2)**			**(CrIS – CERES SNPP) OLR (W/m2)**			**(CERES SNPP – Aqua) OLR (W/m2)**		
	mean	**SD**	**ρ**	**mean**	**SD**	**ρ**	**mean**	**SD**	**ρ**
April 2013	-0.1468	2.4732	0.9980	1.2393	2.2704	0.9984	-1.3861	1.9746	0.9988
April 2014	-0.1428	2.3183	0.9980	0.9891	2.0099	0.9985	-1.1319	1.9033	0.9986
Interannual	-0.0040	3.0705	0.9425	0.2501	2.7127	0.955	-0.2541	1.8827	0.9754

2.6. Practical Considerations

2.6.1. Numerical Computation Considerations

OLR regression coefficients at eight view angle regimes are used to increase computational speed. It is a Pixel by pixel algorithm and it does not require dynamic ancillary input data.

2.6.2. Programming and Procedural Considerations

The OLR shall be generated in the NDE system within 16 minutes of receipt of the input data for NUCAPS. The CrIS OLR software running within NUCAPS shall be able to generate the OLR product using either low or hi-res CrIS SDR data as input. The OLR software will contain range checks to ensure that the OLR data will flag data outside of the range. The CrIS OLR code shall generate Outgoing Longwave Radiation from the CrIS SDR input. The CrIS OLR code shall use static regression coefficients to generate the OLR product. Metadata for the CrIS OLR netCDF files shall be generated for NCEI following existing NDE metadata standards defined in the DAP standards document V1.5. Daily 0.5×2.0 global CrIS OLR grids shall be generated within the NUCAPS software running within NDE and supplied to OSPO for product monitoring. A fully functional pre-operational package shall be created in the Development Environment at STAR. STAR has access to CrIS OLR data from the STAR Collaborative Data Repository (SCDR). The CrIS OLR package will be integrated, run, and tested within NUCAPS at STAR. The Development Environment shall include GNU Fortran and C/C++ compilers version 4.1.2 or greater.

2.6.3. Quality Assessment and Diagnostics

The CrIS OLR package shall have a QC monitoring capability. The CrIS OLR package output shall include overall OLR flux quality control flags. The OLR software will contain range checks to ensure that the OLR data will flag data outside of the range.

2.6.4. Exception Handling

- Quality control flags will be checked and inherited from the sensor input data for handling these exceptions.
- Bad sensor input data (depending on what input QC available)
- Missing sensor input data
- Algorithm can't be run if any of the needed channel data are bad or missing.

2.7. Validation

For validation purposes, we use CrIS sensor data record (SDR) (radiances) and CERES S-NPP FM5 Edition1A SSF and CERES *Aqua* FM3 Edition3A data sets. In this paper, we will present the CrIS OLR estimation algorithm using CrIS pseudo-channel radiances to predict CERES-like OLR.

To validate the accuracy and precision of CrIS derived CERES-like OLR (hereinafter referred to as CrIS OLR), we use available CERES outgoing longwave radiation fluxes from Suomi-NPP (hereinafter referred to as S-NPP CERES OLR) and from Aqua (hereinafter referred to as Aqua CERES OLR) platforms.

– Daily OLR

Our operational CrIS OLR will provide near real-time data daily values with less than 2 hours latency, which is more than adequate for weather/climate applications. The daily OLR data can identify the variations in tropical clouds and rainfall that drive global weather patterns. Simultaneous CERES broadband measurements for S-NPP are the best candidate to validate the CrIS OLR algorithm. However, the amount of available simultaneous measurement for the study is limited; as of the writing of this paper, S-NPP CERES OLR SSF products on NASA ASDC website were only available from January 27, 2012 to June 30, 2014. Also we found the quality flag of the CrIS SDR from Comprehensive Large Array-data Stewardship System (CLASS) is suboptimal (too many cases are flagged as "bad"). We thus requested the NOAA/STAR AIT (Algorithm Integration Team) to reprocess the CrIS SDRs using the newest version of offline ADL (Algorithm Development Library). Due to the difference of the spectral range and spatial resolution of these two instruments, we average CERES and CrIS OLR on a $1^o \times 1^o$ latitude-longitude grid.
Figures 2-3 and 2-4 show the $1^o \times 1^o$ latitude-longitude grid CrIS OLR S-NPP CERES and global distribution on April 26, 2014. Both figures agree well showing geophysically reasonable and spatially consistent patterns.
The larger OLR values over major deserts are due to the desert surface emission, and the OLR values near equator are relatively small due to the high cloud tops associated with the intertropical convergence zone (ITCZ). Note also the large OLR in the vicinity of the oceanic subtropical highs (30^oN and 30^oS), and Antarctica has the coldest and driest climate resulting in the lowest OLR.
Figure 2-5 shows the difference distribution corresponding to Figures 2-3 and 2-4.

The larger value in bias for the ascending orbits is probably the result of solar radiation during daytime reducing the amount of scene uniformity. Other factors include FOV size and view geometry, both of which can affect apparent cloud cover. The large differences occur mostly over land such as Sahara Desert region during the daytime where CrIS OLR presents an overestimation compared with S-NPP CERES OLR. When we compared the Aqua CERES OLR over $1^o \times 1^o$ lat/lon grid on the same day (Apr. 26, 2014), we found Aqua CERES OLR is also overestimated over Sahara compared with S-NPP CERES OLR. Recall that CrIS OLR uses Aqua CERES OLR as its anchor, so similar patterns such as this might be expected.
The NASA CERES team has also reported (private communication) on biases between S-NPP and Aqua CERES OLR, and the differences might result from this systematic bias. The differences might also be caused by the different viewing and scanning properties of CrIS and CERES, and inhomogeneous scenes due to the different spatial resolution between these two instruments. In the midlatitudes over convective areas, the cloud amount and cloud top height might play an important role.

Figure 2-6 shows the histogram of the differences as well as the density-scatterplot of the estimated CrIS OLR and S-NPP CERES OLR on April 26, 2014 for both ascending and descending orbits. The bias is near 1 Wm^{-2} and standard deviation is near 5 Wm^{-2}.

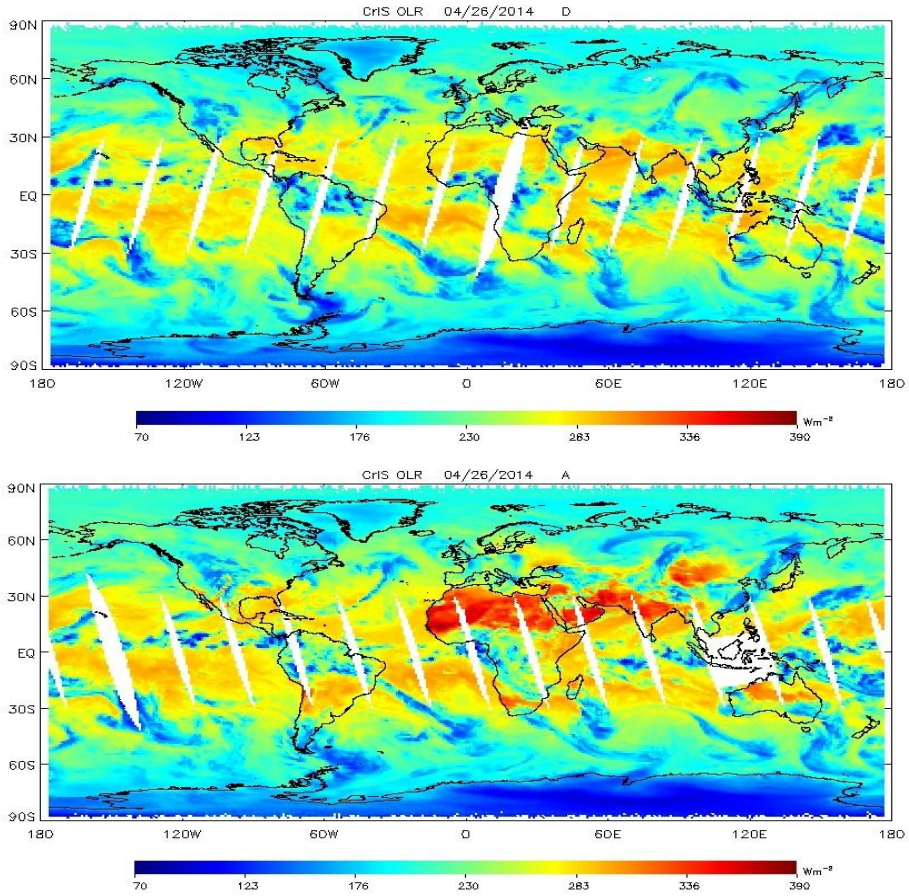

Figure 2-3 Outgoing longwave radiation (OLR, Wm^{-2}) for 26 April 2014, derived from the ascending (top) and descending (bottom) orbits of CrIS measurements.

If we remove less homogeneous scenes, which are decided by the threshold of (CV ≤ 5) for both S-NPP CERES and CrIS OLR data sets on each grid point, and the bias reduces to less than 1 Wm^{-2} and the standard deviation is between 2 and 2.5 Wm^{-2} for the uniform scenes, which might be expected from a smaller OLR spatial variation.

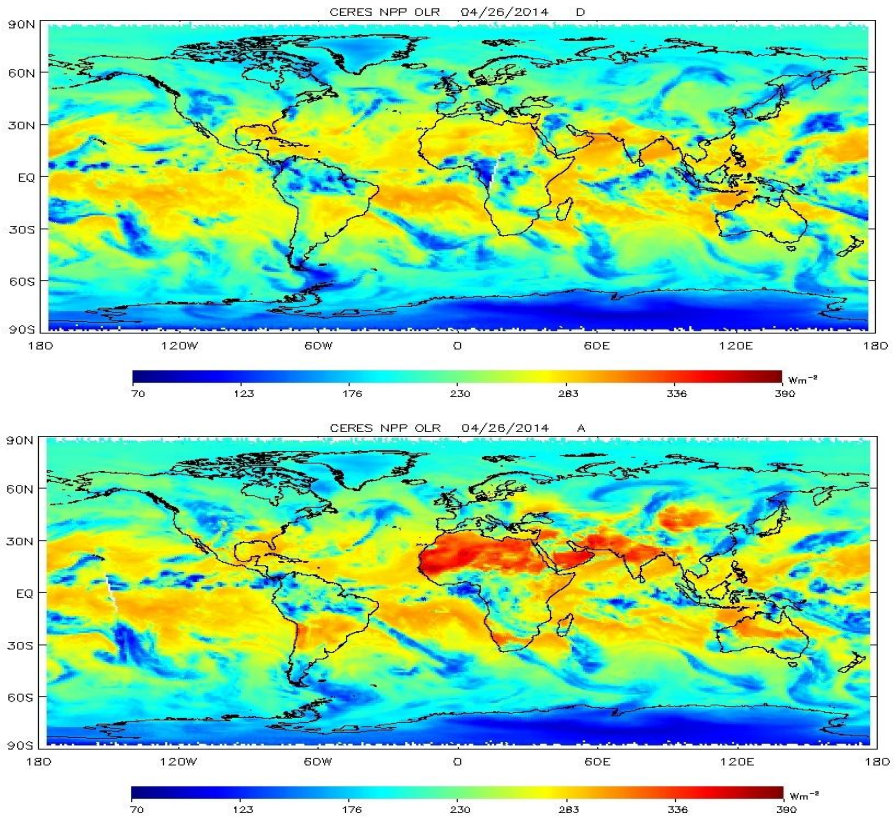

Figure 2-4 Outgoing longwave radiation (OLR, Wm^{-2}) for 26 April 2014, derived from the ascending (top) and descending (bottom) orbits of the S-NPP CERES measurements

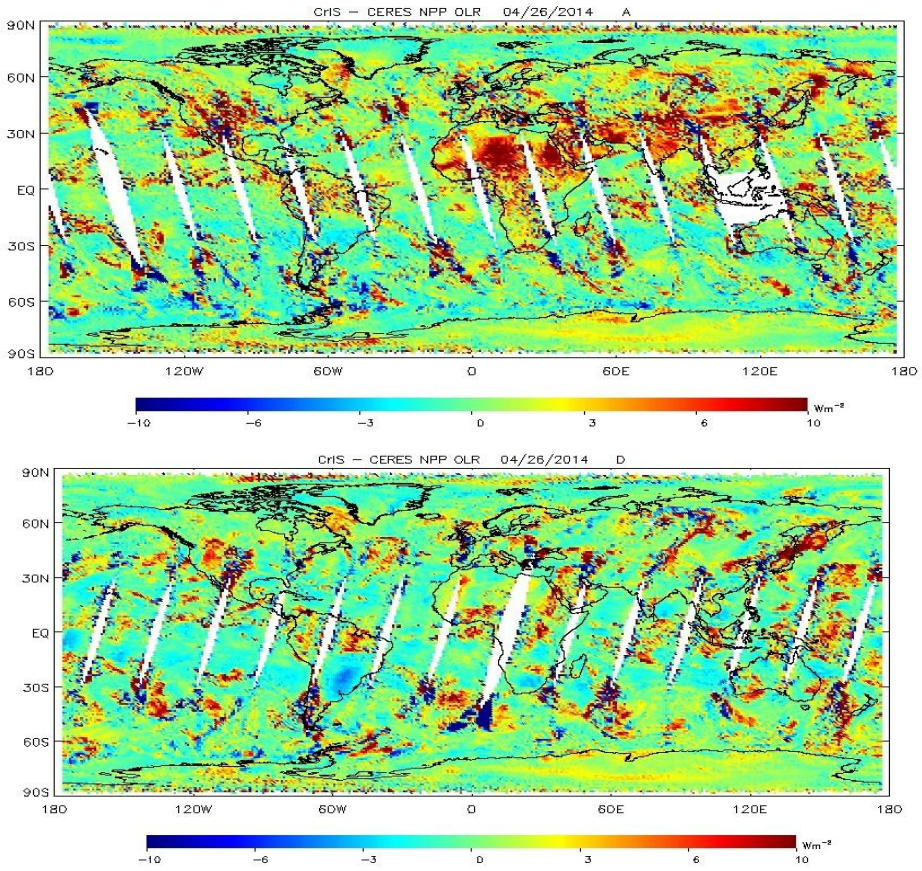

Figure 2-5 Differences (Wm^{-2}) between the CrIS and S-NPP CERES OLR for the ascending (top) and descending (bottom) orbits of 26 April 2014.

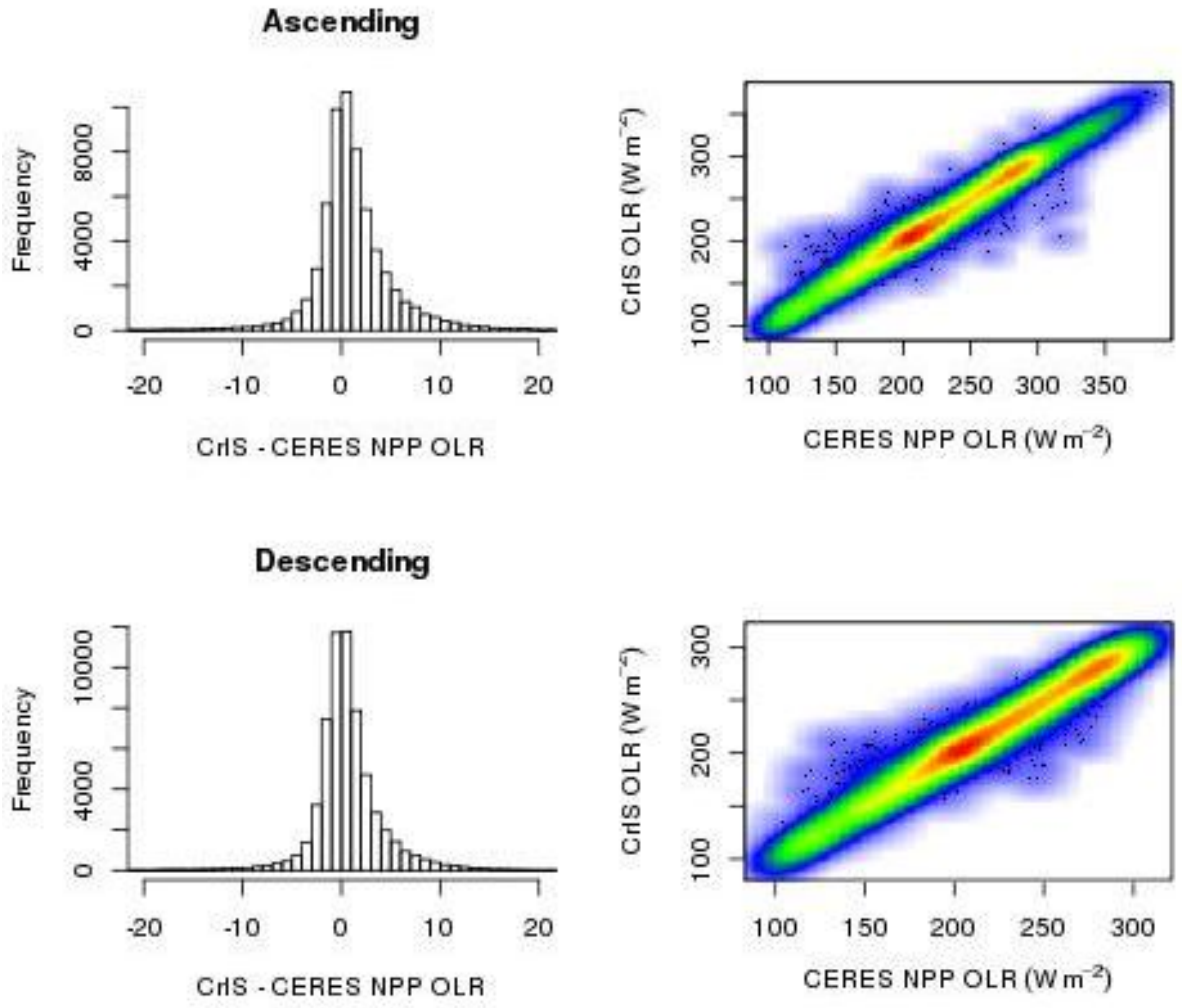

Figure 2-6 Histograms of the differences between the S-NPP CERES OLR and the estimated CrIS OLR for 26 April 2014 (left), together with scatter plots (right). Results of OLR for ascending and descending orbits are shown in the top and bottom panels. The mean and the standard deviation of the differences between these two OLR data sets are 1.138 Wm^{-2} and 4.957 Wm^{-2} for the ascending orbits and 0.624 Wm^{-2} and 4.484 Wm^{-2} for the descending orbits, respectively.

– **Monthly mean and Interannual variability**

Monthly mean fields are important for climate research, and it has been widely used to estimate precipitation. Our operational CrIS OLR product uses CrIS radiance measurements as input with static ancillary data to retrieve CERES-like OLR with 2 hour latency.

It is useful to evaluate CrIS OLR by comparing the monthly mean and interannual variability among those OLR values from different instruments.

We generate OLR monthly means on a $1^o \times 1^o$ global grid by taking the averages of the grid cell values for both ascending and descending orbits each day of a given month for all scenes. Due to the limited CERES S-NPP OLR data sets available and missing granules in CrIS SDR data sets, we calculated monthly means for April 2013 and April 2014 respectively, for S-NPP CERES, Aqua CERES and CrIS derived OLR, and the global distributions are illustrated in Figures 2-7 and 2-8. The interannual variability (difference between April 2013 and 2014) is shown in Figure 2-9, and the ratio between standard deviation of the OLR interannual differences for CrIS and that of Aqua and S-NPP CERES are 0.998 and 0.993 respectively. The ratios indicate that the OLR interannual variability depicted in the CERES is well captured by the CrIS OLR. The global grid comparisons demonstrate that the spatial patterns agree very well and

the spatial correlation is over 99.8% in monthly mean comparisons. The comparison statistical results are summarized in Table 2-4 . It indicates that there is little drift between CrIS's interannual difference and that of CERES Aqua, approximately -0.004 Wm^{-2}. The very small difference of -0.004 is a very important result, and can be attributed to the stability of CERES Aqua. The training dataset was from 2006 between AIRS and CERES, and these results are from April 2013 and 2014.

The CrIS to AIRS adjustment (Eq. 2), which is based on simulated data, introduces no theoretical bias between CrIS and AIRS OLR. Studies have shown biases generally within 0.1 K (brightness temperature) between AIRS, CrIS and IASI with negligible instrument drift. The small bias seen here implies that these hyperspectral infrared sounders provide an effective and highly accurate approach for monitoring OLR. Furthermore, JPSS plans to fly CrIS instruments on a series of JPSS satellites to at least 2038. IASI and the next generation of IASI sensors are slated to operate to at least 2042. OLR from both CrIS and IASI will provide long-term records of OLR for monitoring climate.

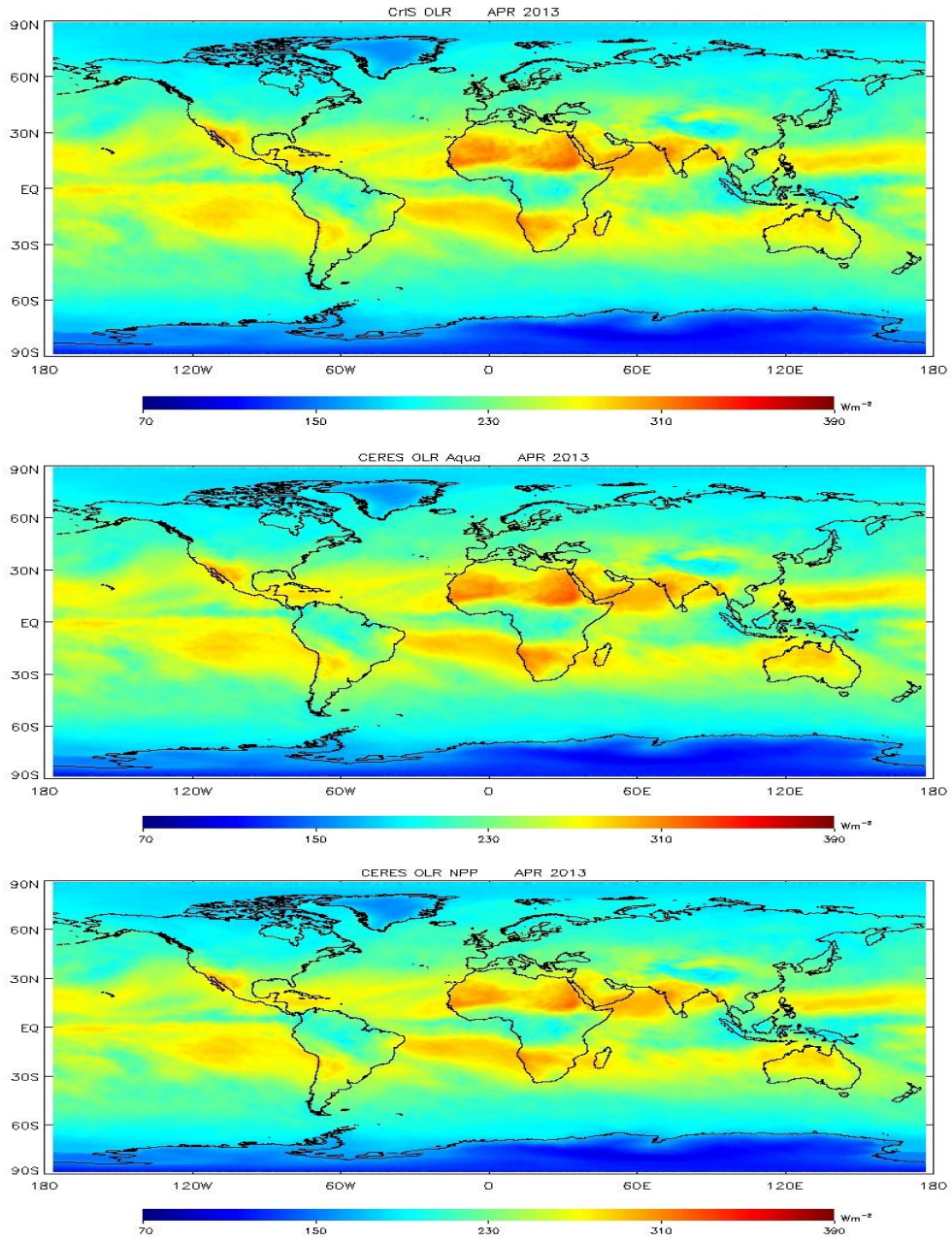

Figure 2-7 OLR monthly mean of April 2013 over $1^{o} \times 1^{o}$ global grids for all scenes. (upper) CrIS derived OLR, (middle) Aqua CERES OLR (lower) S-NPP CERES OLR.

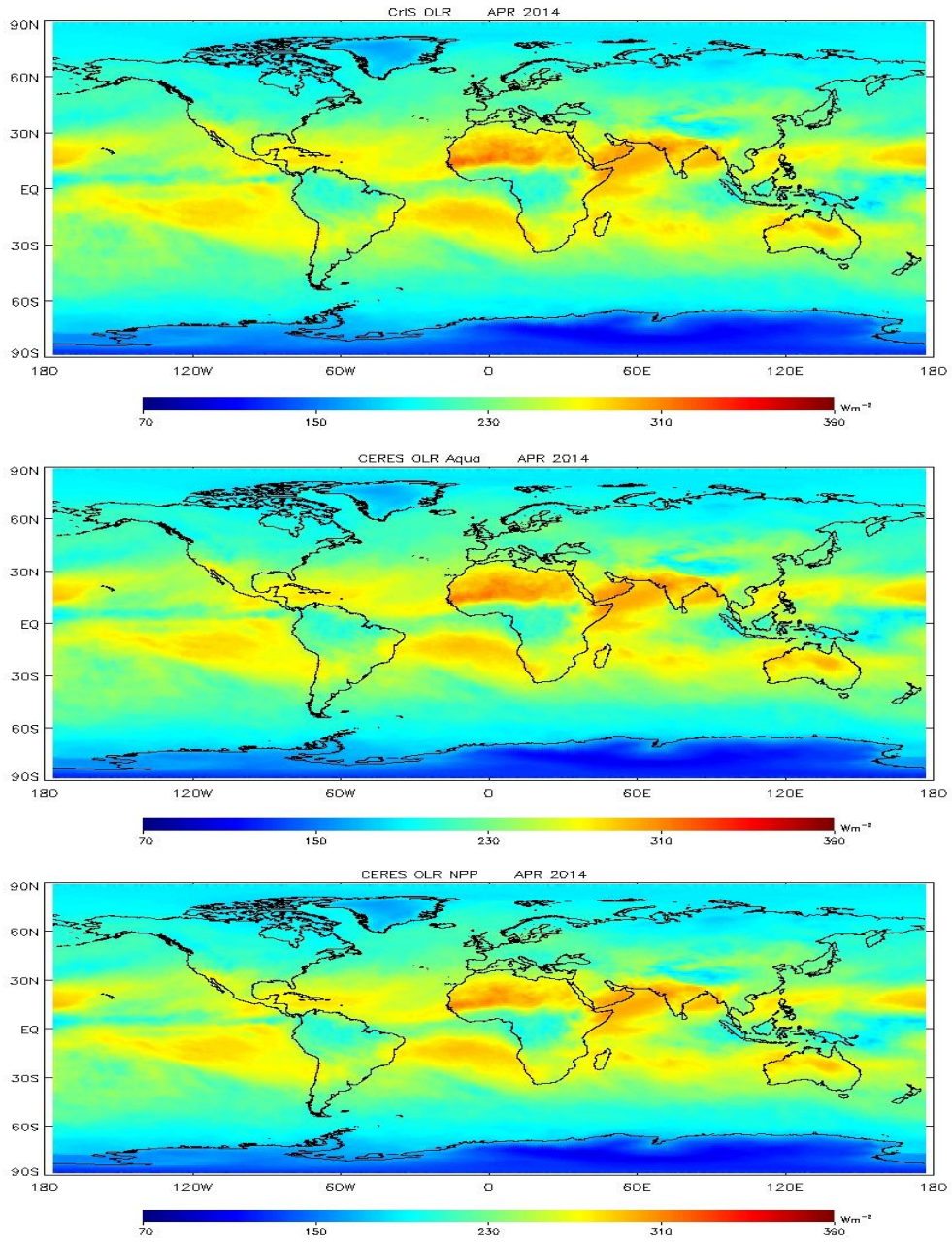

Figure 2-8 OLR monthly mean of April 2013 over $1^{o} \times 1^{o}$ global grids for all scenes. (upper) CrIS derived OLR, (middle) Aqua CERES OLR, and (lower) S-NPP CERES OLR.

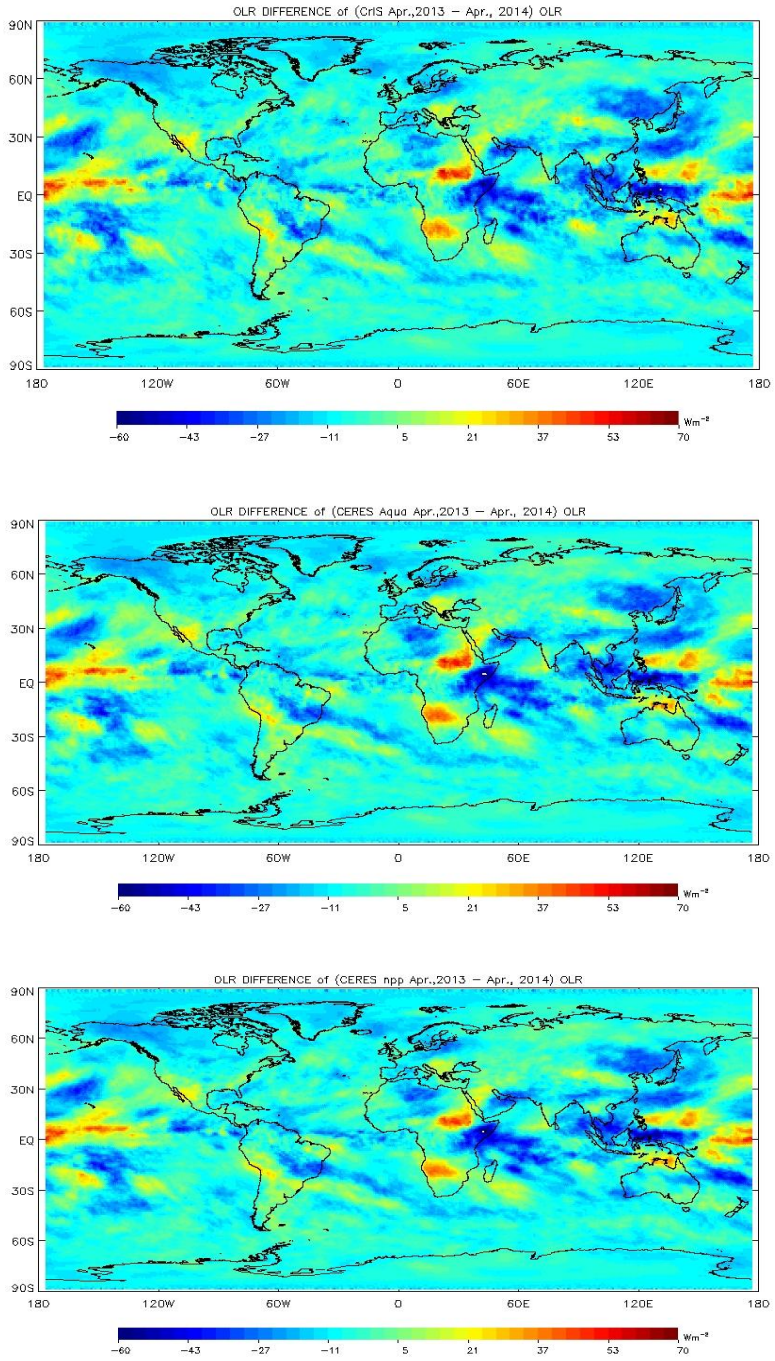

Figure 2-9 Interannual OLR differences between April 2013 and April 2014 over $1^o \times 1^o$ global grids for all scenes. (upper) CrIS derived OLR, (middle) Aqua CERES OLR, and (lower) S-NPP CERES OLR.

3. ASSUMPTIONS AND LIMITATIONS

3.1. Performance Assumptions

– **Assumptions:**

In this work we use CERES Aqua as an absolute reference for all of our hyperspectral IR OLR products, regardless if they are from AIRS, IASI or CrIS, enabling the creation of consistent and stable OLR records from hyperspectral IR sounders.

– **Limitations:**

There are relatively larger biases in the Sahara region and over dry land during daytime. The accuracy of CrIS OLR depends on that of CERES OLR on Aqua and SNPP.

3.2. Potential Improvements

– Re-generate regression coefficients using new version CERES SSF OLR, like CERES Aqua FM3 Edition4A SSF products

– Use SNPP full resolution radiances for OLR estimation

– J-1 full resolution OLR estimation

4. REFERENCES

Sun, F., M. D. Goldberg, X. Liu, and J. J. Bates (2010), Estimation of outgoing longwave radiation from Atmospheric Infrared Sounder radiance measurements, J. Geophys. Res., 115, D09103

Kexin Zhang, Mitchell D. Goldberg, Fengying Sun, Lihang Zhou, Walter W. Wolf, Changyi Tan, Nicholas R. Nalli, and Quanhua Liu, Estimation of Near Real-time Outgoing Longwave Radiation from Cross-track Infrared Sounder (CrIS) Radiance Measurements, submitted to JTECH for review.

END OF DOCUMENT